*Essential Readings in Light Metals: Aluminum Reduction Technology.*
Edited by Geoff Bearne, Marc Dupuis and Gary Tarcy.



# MATHEMATICAL MODELLING OF ALUMINUM REDUCTION CELL POTSHELL DEFORMATION

Marc Dupuis

GéniSim Inc.
3111 Alger St., Jonquière, Québec, Canada, G7S 2M9
marc.dupuis@genisim.com

**Abstract**

One of the key components of an aluminum reduction cell design is the potshell design. The potshell must be designed in such a way that it will not deform excessively in operation and will remain as much as possible in elastic deformation mode. Yet, over-designed potshell are very costly. So, it is important to achieve a design where all sections are getting their fair share of the total load and are being charged close to their elastic limit.

It is obviously impossible to achieve such an optimal potshell design without extensive use of mathematical modeling tools. Three such tools are presented here in order of complexity namely the "empty shell", the "almost empty shell" and the "half empty shell" ANSYS® based thermo-mechanical models. Results are presented for each model, both in elastic and plastic modes, as well as required CPU times.

## Introduction

As quoted in [1], a well-designed shell is supposed to withstand the internal forces induced by thermal and chemical changes in the reduction cell. The thermal changes are quite straightforward to assess if a complementary thermo-electric model is available [2]. The effect of those thermal changes of the cell can be separated into two elements. First, the effect of the thermal changes that occurs in the potshell itself is straightforward to assess. Second, the effect of the thermal changes that occur in the lining: this one is much more difficult to assess due to the complexity of the material properties involved.

As for the chemical changes, they are the consequence of sodium penetration into the carbon cathode blocks. This sodium penetration makes the carbon swell and hence, the cathode blocks expand chemically. Unfortunately, the physic of that chemical expansion is not well understood. The key references on that subjects are Rapoport [3] and Dewing [4]. According to Dewing, the stress-strain relationship of the sodium swelling of the carbon is:

$$\varepsilon = \varepsilon_0 10^{-k\sigma} \qquad (1)$$

where: $\varepsilon$ is the carbon strain at equilibrium

$\varepsilon_0$ is the carbon free expansion strain

$\sigma$ is the compressive stress in the carbon

k is a constant

Furthermore, Dewing [4] has estimated k to be equal to 6.4E-4 when $\sigma$ is expressed in PSI, which corresponds to 0.092825 when $\sigma$ is expressed in MPa. On the other hand, $\varepsilon_0$ the carbon free expansion strain varies a lot depending on the carbon grade and quality. 3% is a typical value for 20% semi-graphitic cathode grade, which is about ten times more that the thermal expansion.

Figure 1 presents the Dewing strain-stress relationship for a cathode block having a 3% free expansion strain. For comparison, a typical thermal expansion strain-stress relationship is also presented.

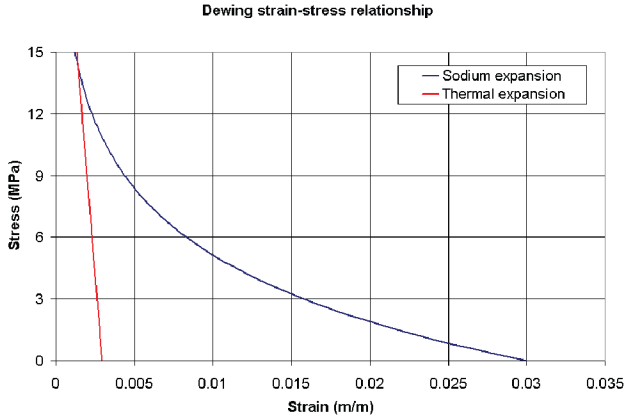


Figure 1: Dewing strain-stress relationship

Dewing [4] has also established the sodium diffusion coefficient to be equal to 4E-5 $cm^2/s$, which corresponds to 3.456E-4 $m^2/day$. Figure 2 presents the corresponding sodium saturation for a typical 45 cm thick cathode block for the full block thickness after 10, 20, 40 and 80 days.

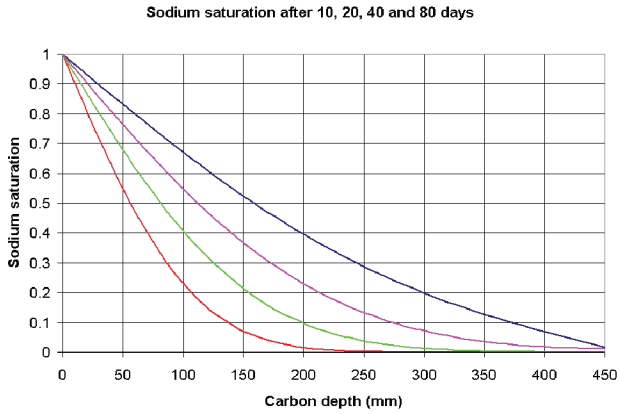


Figure 2: Sodium saturation in a 45 cm cathode block vs. depth

Curves presented in Figure 2 can be obtained by numerically solving the diffusion partial differential equation:

$$\frac{\delta^2 C}{\delta x^2} = \frac{1}{D}\frac{\delta C}{\delta t} \tag{2}$$

Alternatively, it is possible to use the analytical solution of that diffusion equation also presented by Dewing [4]:

$$C = C_0\left\{1 - \frac{4}{\pi}\sum_{n=0}^{\infty}\frac{1}{(2n+1)}\sin\left[\frac{(2n+1)\pi x}{2h}\right]\exp\left[-\left(\frac{(2n+1)\pi}{2n}\right)^2 Dt\right]\right\} \tag{3}$$

Figure 3 presents the corresponding sodium saturation for the same typical 45 cm thick cathode block, this time at x = ¼, ½ and ¾ of the total block thickness as function of time as computed by Equation 3. Figures 2 and 3 show that it takes about 80 days for the sodium diffusion front to reach the bottom of the cathode block and about 1000 days for the cathode block to be fully saturated in sodium from top to bottom.

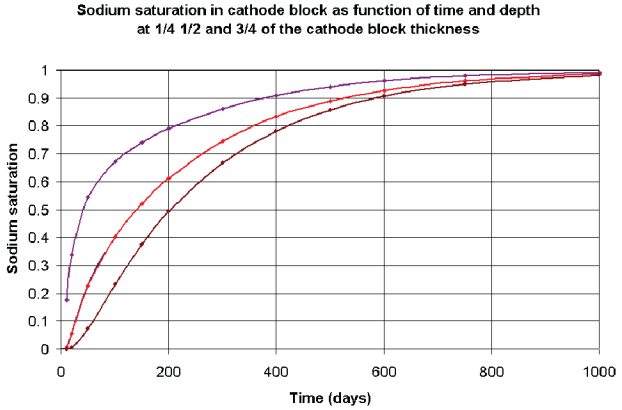


Figure 3: Sodium saturation in a 45 cm cathode block vs time

In summary, the potshell needs to withstand from start-up time the internal forces induced by the thermal changes and in addition, gradually over a period of about 1000 days, the internal forces induced by the chemical changes. To complicate further the matter, the intensity of those internal chemical forces will depend on the rigidity of the potshell structure itself.

## Historical background

Considering all this, various types of mathematical modeling tools have been developed in order to assist potshell design optimization work. The ideal situation should allow to include all the physics described above in a comprehensive model and to obtain fast and accurate predictions from it. Speed, in addition to accuracy, is required to be able to use any model to analyze various design proposals relatively efficiently and hence converge on the optimum potshell design in an acceptable time frame.

Historically, this type of model was developed in the late 80's at Alcan International by a group of experts under the leadership of the author. Unfortunately, not much of that huge R&D effort was published at that time. Yet, Read [5] presented that model at a 1990 supercomputer symposium in Montreal. Figure 1 of [5] shows that the model includes the potshell and about half of the lining material. Only the lining material directly under the cathode blocks is left out of the model geometry. For reason that will soon become obvious, we shall name that type of model the "half empty shell" type of model. The fact that that model was presented in a supercomputing symposium and that we can read in [5] that "the computational task, even in CRAY terms, is staggeringly large" clearly indicates that the hope to be able to use that type of model as an efficient design tool was not achieved at the time.

On the other end of the spectrum, also historically, the "empty shell" type of model was successfully being used to improve existing potshell design as reported in [6] or to quickly analyze potshell design options like in [7] per example. As its name indicates, that type of model only represents the geometry of the potshell itself, which contribute to significantly reduce the computational requirements. Yet, as it rely on an assumed internal load, that type of model cannot take into account the relationship that exist between the potshell rigidity and the intensity of the internal forces.

This is why a third type of model has been developed in the early 90's [1,8]. In that type of model, the lining material between the potshell and the cathode blocks is represented in addition to the potshell itself hence the name "almost empty shell". In that third type of model, instead of using an assumed internal load, an iterative process ensures that the imposed internal load lies exactly on the Dewing strain-stress relationship automatically ensuring that a more rigid potshell is getting a larger internal load.

Almost 20 years after the initial development of these three types of potshell mechanical models, hardware capabilities have increased radically. A model that was way to big to be considered an efficient design tool at the time might become practical. For that reason, it is a good thing to revisit those three types of potshell mechanical models and reassess their relative merits as efficient potshell design tools.

## "Empty shell" potshell model

The "empty shell" thermo-mechanical potshell model, like the other two types of models for that matter, is based on the usage of the quadrilateral Finite Strain shell element (SHELL181) in the commercial code ANSYS® [7]. The temperature distribution obtained from the full cell quarter thermo-electric model [2] is applied as a body load to the entire potshell structure. Also for all three types of model, it is possible to solve the mechanical problem only by considering the elastic properties of the potshell steel structure or to consider in addition the temperature dependent isotropic hardening von Mises plasticity behavior of the potshell steel structure using the MISO non-linear hardening option in ANSYS® [7].

All this is relatively straightforward to setup, but there is still the internal forces generated from the thermal and chemical lining expansion to be specified as boundary conditions in the model. Obviously, model boundary conditions are model inputs, while those internal forces are *a priori* unknown and depend on the potshell structural rigidity. The historical approach to this problem is to rely on a database of past model validation exercises to define an internal pressure (or forces) loading scheme based on the cathode block size and position relative to the potshell. That loading scheme is at best semi-empirical and is typically considered as a trade secret, so it is never presented in publications.

Of course, having to prescribe the value of the internal pressure (or forces) loading as boundary conditions, regardless of the quality and quantity of previous field measurement campaigns and

subsequent model validation exercises, is a serious weakness. The internal forces that will develop in a new potshell and lining design will depend on that new potshell structural rigidity, on the sodium swelling characteristics of the grade of cathode blocks selected, and on the materials between the blocks and the potshell as previously discussed.

It may be a serious disadvantage, but the corresponding advantage is the fact that this type of model can be solved much more rapidly than the other two types of potshell mechanical models available. Per example, the "empty shell" demo potshell model using only elastic steel properties presented in Figure 4 took only 150 CPU seconds to solve on a 64 bits dual core Intel Centrino T9300 Dell Precision M6300 portable computer running ANSYS® 11.0 version.

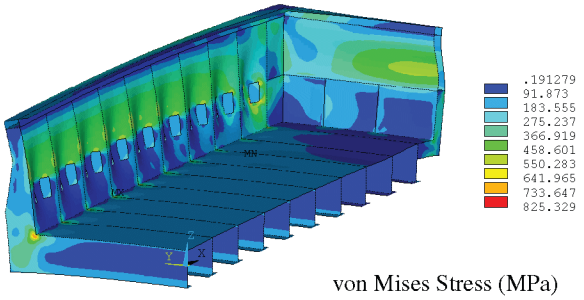


von Mises Stress (MPa)

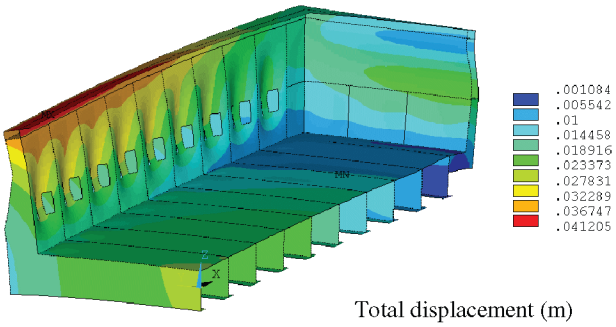


Total displacement (m)

Figure 4: Elastic mode "empty shell" demo potshell model

The "empty shell" demo potshell model using elasto-plastic steel properties presented in Figure 5 took 11 times more CPU to solve, but still this is only 1706 CPU seconds or 28 CPU minutes.

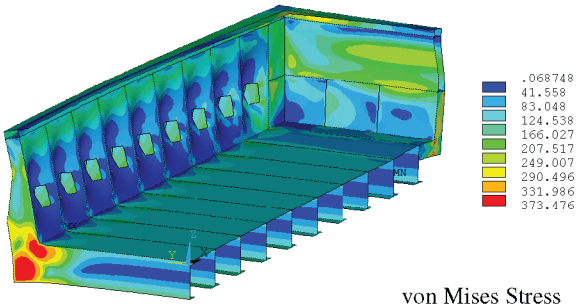


von Mises Stress

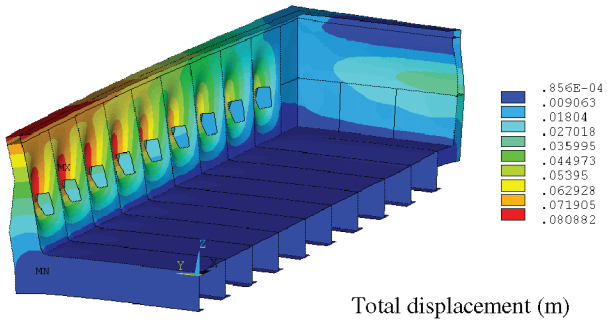


Total displacement (m)

Figure 5: Plastic mode "empty shell" demo potshell model

**"Almost empty shell" potshell model**

Clearly, a 30 minutes response time is not a problem, so the "empty shell" potshell model would be the perfect design tool if we could trust that the appropriate internal loads have been applied and hence that the correct potshell deflection has been calculated.

This relatively small turnaround time is opening the door to the option of spending more CPU time in order to increase the accuracy of the model prediction and still having an efficient design tool. In the "almost empty shell" model type, this is achieved by adding the lining geometry between the potshell walls and the cathode blocks all around the potshell and by applying a pressure loading as boundary condition at the carbon block/side lining interface that is lying on the Dewing strain-stress relationship (i.e. that represents the carbon block equilibrium condition). In order to be able to do so, a new convergence numerical scheme external to the ANSYS solver must be setup [1]. Starting from an assumed initial internal load, the task of that external convergence loop is to converge toward that cathode block equilibrium condition pressure loading for each element face of the carbon block/side lining interface.

It turns out that that can be achieved by using an under-relaxation numerical scheme in about 20 iterations adding about the same factor to the "almost empty shell" type model solution time compared to the "empty shell" type model. Per example, the "almost empty shell" demo potshell model solved in elastic properties mode presented in Figure 6 took 3898 seconds CPU or 65 minutes CPU to solve while the "almost empty shell" demo potshell model solved in plastic properties mode presented in Figure 7 took 27524 seconds CPU or 7.6 hours CPU to solve.

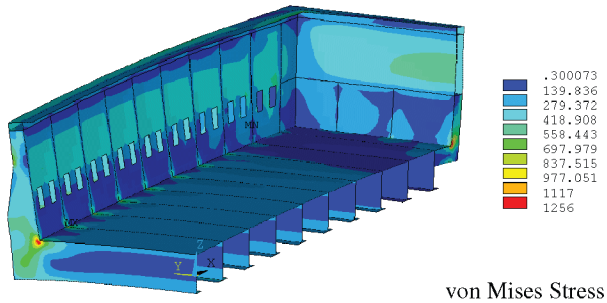


von Mises Stress

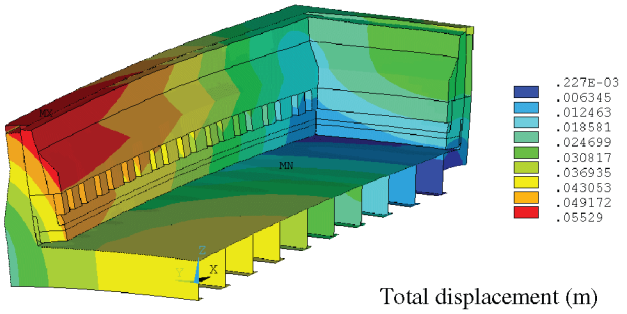


Figure 6: Elastic mode "almost empty shell" demo potshell model

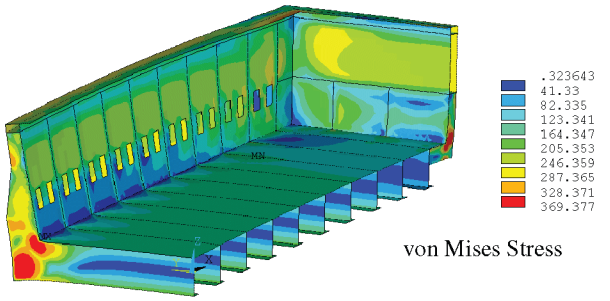


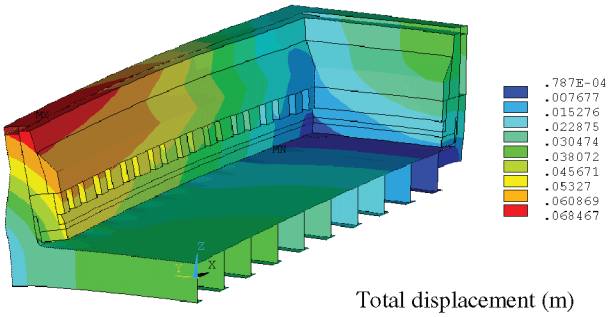


Figure 7: Plastic mode "almost empty shell" demo potshell model

It is interesting to notice that there is a lot less difference between the potshell deflection of the elastic and plastic properties modes results in the case of the "almost empty shell" model type as compared to the "empty shell" model type. This result can easily be explained by the fact that the internal load of the "almost empty shell" model type has automatically adjusted itself proportionally to the potshell structure rigidity has it can be seen in Figures 8 and 9.

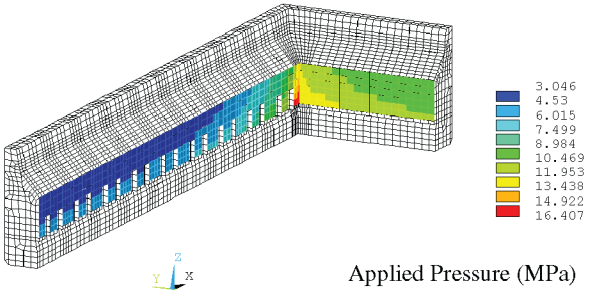


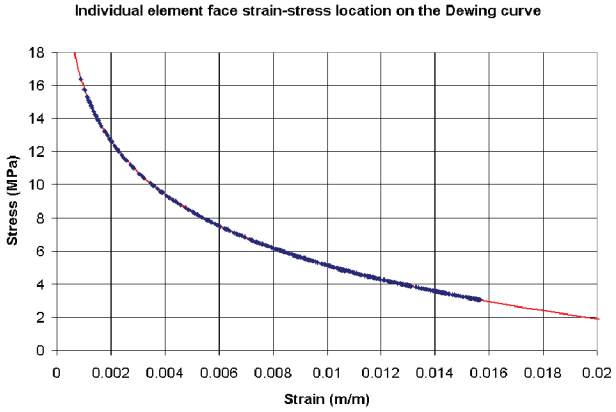


Figure 8: Elastic mode "almost empty shell" internal pressure load

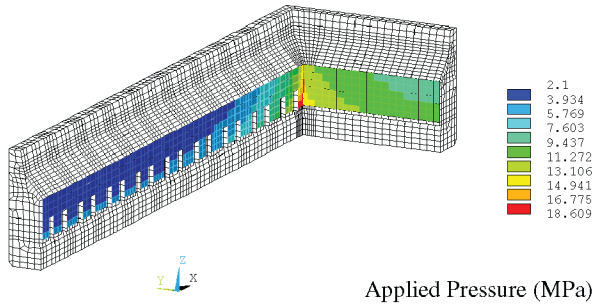


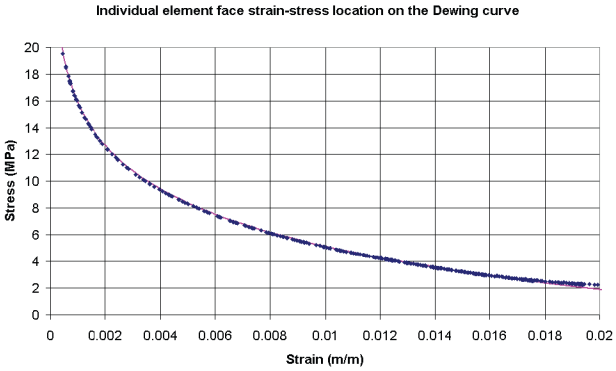


Figure 9: Plastic mode "almost empty shell" internal pressure load

An overnight turn-around time is certainly not as convenient as a 30 minutes one, but it might be well worth if the accuracy of the model prediction and hence the model reliability as a design tool is significantly increased.

### "Half empty shell" potshell model

Historically, the "almost empty shell" potshell model type has been developed after the "empty shell" and the "half empty shell" potshell model types as a compromise between model turn-around time and model accuracy. At the time, the potshell model type that was considered as the most accurate, the "half empty shell" potshell model was taking far too much CPU time to solve even on expensive supercomputer. Today, despite the success of the "almost empty shell" potshell model type to offer that compromise, it is a good time to reevaluate the value of the "half empty shell" potshell model type as a design tool.

In addition to the lining material located between the potshell walls and the cathode carbon blocks already present in the "almost empty shell" potshell model type, the "half empty shell" potshell model type also includes the geometry of the cathode blocks themselves. As already briefly described in [5], the Dewing sodium expansion behavior of the cathode blocks is treated in ANSYS® as a "creep-like" behavior. By definition, this means that it is required to solve that model in transient mode following the build-up of the sodium concentration in the cathode blocks from start-up to around 1000 days of operation where the cathode blocks get fully saturated in sodium. This way, the model computes the incremental build-up of the strain-stress relationship due to the gradual and non-uniform carbon swelling generated from the gradual increase in the sodium concentration in the cathode blocks and also to the gradual and non-uniform restraining effect of the potshell on the cathode blocks sodium expansion. Of course, this must be done using relatively small time steps hence the huge CPU time requirement.

The setup of the model in ANSYS® and the optimization of the time steps size represent a serious model development and testing effort, yet fortunately, the bulk of the R&D model development work had already been done about 20 years ago! Reference [5] reports 90 MFLOPS of sustained performance on solving such a model using ANSYS® 4.4a on a CRAY X-MP/24. We can now report 6000 MFLOPS of sustained performance while solving a similar model using the SPARSE solver available in ANSYS® 11 on the 64 bits dual core Intel Centrino T99300 Dell Precision M6300 portable computer. This huge increase in MFLOPS is due to improvements in both the hardware and the software side. On the software side, Reference [5] reports delays caused by huge I/O activities and corresponding huge I/O wait time. With the use of the SPARSE solver available in ANSYS® 11.0, it is possible to solve the model in-core using 2.4 GB of RAM out of the 4.0 GB of RAM available on the computer. Furthermore, because it is a dual core computer and ANSYS® solver is using both processors, the CPU time and elapse time are about equal most of the time.

Despite the software side improvements, solving a "half empty shell" potshell model still requires a lot of computer power, clearly, all the computing resources available on the Dell M6300 were required. Solving the "half empty shell" demo potshell model in elastic properties mode presented in Figure 8 took 25,335 CPU seconds or 7.0 CPU hours which is 6.5 times more than what was required to solve the "almost empty shell" demo potshell model in elastic properties mode. Solving the "half empty shell" demo potshell model in plastic properties mode presented in Figure 9 took 103842 CPU seconds or 1.2 CPU days which is 3.8 times more than what was required to solve the "almost empty shell" demo potshell model in plastic properties mode. It is interesting to note that the CRAY X-MP/24 would have required about 80 CPU days to solve the save model at 90 MFLOPS, which could explain why Figure 1 of [5] presents model results after 60 days of cathode life only!

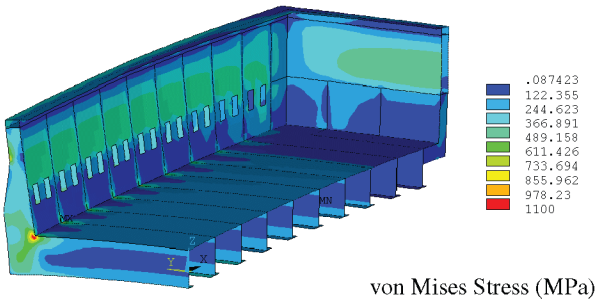


von Mises Stress (MPa)

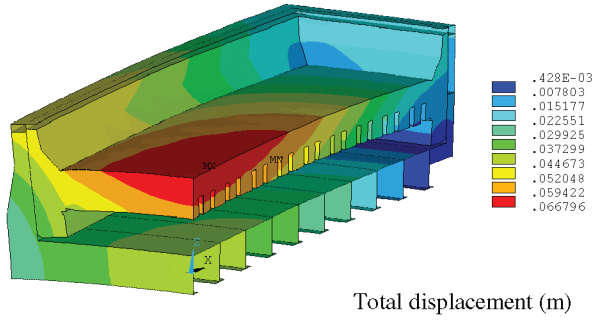


Total displacement (m)

Figure 8: Elastic mode "half empty shell" demo potshell model

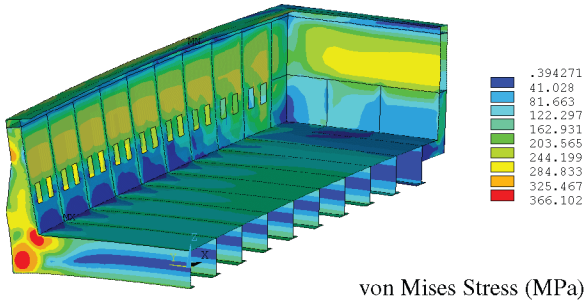


von Mises Stress (MPa)

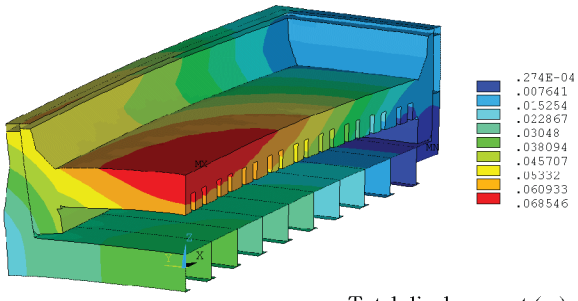


Total displacement (m)

Figure 9: Plastic mode "half empty shell" demo potshell model

Both in elastic and in elasto-plastic property mode, the results of the "almost empty shell" and the "half empty shell" potshell model are quite similar, yet, in both cases, the "half empty shell" potshell model predicts less side deflection because the "half empty shell" model type also predicts a significant cathode panel upward deflection accommodating part of that cathode panel expansion which is of course not accounted for by the "almost empty shell" model type. It is important to point out that that cathode panel upward deflection has an impact on the MHD cell stability as demonstrated in [9] and only the solution of an "half empty shell" potshell model type generates the data required to account for that cathode panel upward deflection in the MHD cell stability model.

## Conclusions

Three types of ANSYS® based thermo-mechanical potshell models have been presented and described in details. Nowadays, all three types of models can be used as potshell design tools.

The "empty shell" potshell model type has by far the fastest turn around time which is very convenient to be able to quickly investigate potshell design alternatives. Unfortunately, its ability to make accurate predictions outside of the narrow range of conditions where it has been validated is very questionable.

The "almost empty shell" potshell model type is offering a much wider applicability range as it will automatically adjust the internal load as function of the grade of cathode blocks selected and of the rigidity of the potshell structure. Still, by avoiding to simulate the 1000 days gradual sodium diffusion and gradual carbon swelling in a transient solution, it offers an overnight turn-around time for a very little loss of accuracy.

The "half empty shell" potshell model type is the most accurate model type of the three presented because it incorporates all the known physics of the cathode block sodium expansion phenomena affecting the potshell deformation in addition to the thermal expansion. Still, the accuracy of the third model type is not absolute because even more complex phenomena could be added to the model as discussed in [10] and [11] per example. In particular, the complex behavior of the ramming paste in the big joint during the preheat and early operation period, completely neglected in the current study, would affect the predicted potshell displacement.

Yet, adding even more complex phenomena will further increase the model turn-around time which at 1.2 CPU days is already exceeding the overnight turn-around time that could be considered as the practical upper limit for an efficient design tool, at least when using a 64 bits dual cure Intel Centrino T9300 Dell Precision M6300 computer as the number cruncher.

Finally, until the day where the turn-around time of the "half empty shell" potshell model type would be reduced to mere minutes as it will become maybe 20 years from now (after all it was 80 days on a CRAY X-MP/24 supercomputer 20 years ago), it could be argued that all three types of potshell models have their places in the potshell designer toolbox as sometimes turn-around time matter more than accuracy and sometimes not.

## Acknowledgements

The author wishes to thanks Dr Daniel Richard of Hatch and Mr Lalit Mishra of Dubal for their much needed assistance in using ANSYS® 11.0 thermo-mechanical features, especially in plastic properties mode.

## References

1. G. V. Asadi, M. Dupuis and I. Tabsh, "Shell Design Technique Considering the Sodium Swelling Phenomena of Carbon Cathode Blocks", *in Proceedings of the 32nd Conference of Metallurgists, CIM*, (1993), 125-130.

2. M. Dupuis, V. Bojarevics and J. Freibergs. "Demonstration Thermo-Electric and MHD Mathematical Models of a 500 kA Al Electrolysis cell", *in Proceedings of the 42nd Conference on Light Metals, CIM*, (2003), 3-20.

3. M. B. Rapoport and V. N. Samoilenko, "Deformation of Cathode Blocks in Aluminium Reduction Cells during Process of Electrolysis", *in TsvetnyeMetally,* (1957), vol 30, 44-51.

4. E. W. Dewing, "Longitudinal Stress in Carbon Lining Blocks Due to Sodium Penetration", *in Proceedings of TMS Light Metals,* (1974), vol 3, 879-887.

5. C. M. Read, A. M. Kobos, M. Dupuis, G. V. Asadi and K. P. Misegades, "Modelling of Aluminium Production Processes with CRAY supercomputers", *in Supercomputing Symposium '90,* (1990).

6. M. Dupuis, G. V. Asadi, C. M. Read, A. M. Kobos and A. Jakubowski. "Cathode Shell Stress Modeling", *in TMS Light Metals*, (1991), 427-430.

7. M. Dupuis and D. Richard, "Study of the Thermally-Induced Shell Deformation of High Amperage Hall-Héroult Cells", *in Proceedings of COM*, (2005), 35-47.

8. M. Dupuis, G. V. Asadi, C. M. Read and I. Tabsh, "Hall-Héroult Cell, Cathode Modelling; Impact of Sodium Swelling on the Loading Forces", *in Proceedings of the 31st Conference of Metallurgists, CIM*, (1992), 115-130.

9. M. Dupuis, V. Bojarevics and D. Richard, "Impact of the Vertical Potshell Deformation on the MHD Cell Stability Behavior of a 500 KA Aluminum Electrolysis Cell", *in TMS Light Metals*, (2008), 409-412.

10. G. D'Amours, M. Fafard, A. Gakwaya and A. Mirchi. "Multi-Axial Mechanical Behavior of the Carbon Cathode : Understanding, Modeling and Identification", *in TMS Light Metals*, (2003), 633-639.

11. D. Richard, G. D'Amours, M. Fafard, and M. Désilets. "Development and Validation of a Thermo-Chemo-Mechanical Model of the Baking of Ramming Paste", *in TMS Light Metals,* (2005), 733-738.

# Recommended Reading


Aaberg, R.J., et al. The gas under anodes in smelting cells. Part II: Gas volume and bubble layer characteristics (1997, pp. 341–346).

Ahmed, H.A., et al. Prediction of the thermal aspects of egyptalum prototype high-amperage pre-baked aluminium reduction cells (1994, pp. 333–338).

Antille, J., and R.von Kaenel. Busbar optimization using cell stability criteria and its impact on cell performance (1999, pp. 165–170).

Arkhipov, G.V., and A.V. Rozin. The aluminum reduction cell closed system of 3D mathematical models (2005, pp. 589–592).

Arkhipov, G.V., et al. Simulation of cell thermoelectric field with consideration of electrochemical processes (2007, pp. 327–331).

Barantsev, A.G., et al. Model of process of electrolyses (2000, pp. 315–321).

Bielder, P., and L. Banta. Analysis and correction of heat balance issues in aluminum reduction cells (2003, pp. 441–447).

Bojarevics, V., and K. Pericleous. Comparison of MHD models for aluminium reduction cells (2006, pp. 347–352).

Bojarevics, V., and K. Pericleous. Solutions for the Metal-Bath Interface in Aluminium Electrolysis Cells (2009, pp. 569–574).

Bojarevics, V., and A. Roy. Bubble transport by electro-magnetophoretic forces at anode bottom of aluminium cells (2011, pp. 549– 554).

Bos, J., et al. Numerical simulation tools to design and optimize smelting technology (1998, pp. 393–401).

Bruggeman, J.N., and D.J. Danka. Two-dimensional thermal modeling of the Hall-Heroult cell (1990, pp. 203–205).

Chen, J.J.J., et al. A study of cell ledge heat transfer using an analogue ice-water model (1994, pp. 285–293).

Chesonis, D.C., and A.F. LaCamera. The influence of gas-driven circulation on alumina distribution and interface motion in a Hall-Heroult cell (1990, pp. 211–220).

Descloux J., M. Flueck, and M.V. Romerio. Stability in aluminium reduction cells: A spectral problem solved by an iterative procedure (1994, pp. 275–281).

Descloux, J., and M.V. Romerio. On the analysis by perturbation methods of the anodic current fluctuations in an electrolytic cell for aluminium (1989, pp. 237–243).

Dupuis, M., and V. Bojarevics. Busbar sizing modeling tools: comparing an ANSYS® based 3D model with the versatile 1D model part of MHD-Valdis (2006, pp. 341–346).

Dupuis, M., V. Bojarevics, and J. Freilbergs. Demonstration thermo-electric and MHD mathematical models of a 500 kA aluminum electrolysis cell: Part 2 (2004, pp. 453–459).

Fraser, K.J., et al. Some applications of mathematical modelling of electric current distributions in hall heroult cells (1989, pp. 219–226).

Fraser, K.J., M.P. Taylor, and A.M. Jenkin. Electrolyte heat and mass transport processes in Hall Heroult electrolysis cells (1990, pp. 221–226).

Haugland, E., et al. Effects of ambient temperature and ventilation on shell temperature, heat balance and side ledge of an alumina reduction cell (2003, pp. 269–276).

Holt, N.J., et al. Ventilation of potrooms in aluminium production (1999, pp. 263–268).

Hyde, T.M., and B.J. Welch. The gas under anodes in aluminium smelting cells. Part 1: measuring and modeling bubble resistance under horizontally oriented electrodes (1997, pp. 333–340).

Kiss, L.I., S. Poncsak, and J. Antille. Simulation of the bubble layer in aluminum electrolysis cells (2005, pp. 559–564).

Maarschalkerwaard, A. The use of CFD simulations to optimise ventilation of potrooms (2010, pp. 423–426).

McMinn, C. Energy balance of aluminum reduction cells (1975, Vol.1, pp. 65–76).

Meijer, M. New logistic concepts for 400 and 500 kA smelters (2010, pp. 345–348).

Pfundt, H., D. Vogelsang, and U. Gerling. Calculation of the crust profile in aluminium reduction cells by thermal computer modelling (1989, pp. 371–377).

Pires, R., et al. Integrated approach for safe and efficient plant layout development (2011, pp. 437–441).

Potocnik, V., and F. Laroche. Comparison of measured and calculated metal pad velocities for different prebake cell designs (2001, pp. 419–425).

Purdie, J.M., et al. Impact of anode gas evolution on electrolyte flow and mixing in aluminium electrowinning cells (1993, pp. 355–360).

Robl, R.F. Influence by shell steel on magnetic fields within Hall-Heroult cell (1978, Vol. 1, pp. 1–13).

Romerio, M.V., et al. Determination and influence of the ledge shape on electrical potential and fluid motions in a smelter (2005, pp. 461–468).

Schmidt-Hatting, W., et al. Heat losses of different pots (1985, pp. 609–624).

Segatz, M., and D. Vogelsang. Effect of steel parts on magnetic fields in aluminium reduction cells (1991, pp. 393–398).

Segatz, M., et al. Modelling of transient magneto-hydrodynamic phenomena in Hall-Heroult cells (1993, pp. 361–368).

Sele, T. Instabilities of the metal surface in electrolytic cells (1977, Vol. 1, pp. 7–24).

Severo, D.S., et al. Modeling magnetohydrodynamics of aluminum electrolysis cells with ANSYS and CFX (2005, pp. 475–480).

Shcherbinin, S.A., A.V. Rozin, and S.Y. Lukashchuk. The 3D modeling of MHD-stability of aluminum reduction cells (2003, pp. 373–377).

Solheim, A., and J. Thonstad. Model cell studies of gas induced resistance in Hall Heroult cells (1986, pp. 397–403).

Solheim, A., et al. Gas driven flow in Hall-Heroult cells (1989, pp. 245–252).

Solinas, G.A. Advanced mathematical models for the calculation of magnetic fields in aluminum reduction cells (1978, Vol. 1, pp. 15–42).

Solinas, G.A. Automatic plotting as an effective aid for theoretical studies on reduction cell phenomena (1980, pp. 243–272).

Sulmont, B., and G. Hudault. Application of a thermoelectric model to the investigation of reduction cell thermal equilibrium (1978, Vol. 1, pp. 73–86).

Taylor, M.P., et al. The dynamics and performance of reduction cell electrolytes (1990, pp. 259–266).

Toia, G., U. Florenzani, G. Soletta, and A.Z. Rossi. Application of a mathematical model to ensure optimum potshell design (1979, pp. 495–516).

Tvedt, T., and H.G. Nebell. Newbus, a similation program for calculation of the current distribution in the bus bar system of alumina reduction cells (1988, pp. 567–573).

Urata, N., Y. Arita, and H. Ikeuchi. Magnetic field and flow pattern of liquid aluminum in the reduction cells (1975, Vol. 1, pp. 233–250).

Vershenya, A., et al. Modern design of potroom ventilation (2011, pp. 531–535).

Walker, M.L. Visualisation of tapping flows (1997, pp. 215–219).

Wei, C.C., et al. Modelling of dynamic ledge heat transfer (1997, pp. 309–316).

Yamazaki, K., and K. Arai. Heat balance and thermal losses in advanced prebake anode cells (1975, Vol. 1, pp. 193–214).